Regular Article

PHYSICAL CHEMISTRY RESEARCH
Published by the
Iranian Chemical Society
www.physchemres.org
info@physchemres.org

***Phys. Chem. Res.**, Vol. 6, No. 4, 713-720, December 2018*
DOI: 10.22036/pcr.2018.132220.1486

Fe-Loaded CeO_2 Nanosized Prepared by Simple Co-Precipitation Route

M. Farahmandjou* and M. Dastpak
Department of Physics, Varamin Pishva Branch, Islamis Azad University, Varamin, Iran
(Received 2 June 2018, Accepted 2 August 2018)

FeCe nanoparticles were synthesized by simple co-precipitation method using Iron chloride hexahydrate ($FeCl_3.6H_2O$) and cerium chloride ($CeCl_2{\cdot}5H_2O$) as precursors in the presence of cetyltrimethylammonium bromide (CTAB) surfactant. The samples were characterized by high resolution transmission electron microscopy (HRTEM), field emission scanning electron microscopy (FESEM), X-ray diffraction (XRD), vibration sampling magnetometer (VSM), electron dispersive spectroscopy (EDS) and Fourier transform infrared spectroscopy (FTIR) at different temperatures. The XRD results showed that Fe-doped CeO_2 was single-phased with a cubic structure. SEM images showed the rod-shaped particles of as-prepared sample in the range size of 40-80 nm and annealed smallest one around 15 nm in diameter at 500 °C for 3 h. The TEM studies revealed the squared-like shaped nanosized particles. The sharp peaks in the FTIR spectrum determined the element of Fe-Ce nanoparticles. The EDS spectra showed peaks of iron and cerium with less impurity in the prepared samples. The result of magnetic measurements showed a coercive field and saturated magnetization around 1650 G and 0.04 emu g^{-1} for as-prepared samples, respectively.

Keywords: Fe dopant, Cerium oxide nanocrystals, CTAB, Co-precipitation, Surfactant

INTRODUCTION

In recent times, metal oxide nanoparticles have found many applications in the fields of optics, electronics and medicine [1-18]. In recent years, CeO_2/Ceria nanoparticles have been widely considered in various industries. Among the most important series of applications, light absorber and filter, gas sensor, catalyst in oxidation and fuel cell have been mentioned [19,20]. Cerium oxide materials have the cubic fluorite crystal structure [21]. This material has the ability to conduct oxygen as a result of its capacity and ability to change (Ce^{3+}/Ce^{4+}). Therefore, it exhibits good catalytic properties. Ceria ceramic materials have been widely studied due to the low ionic conductance of oxygen at low temperatures [22]. However, the wide band of CeO_2 (3.22 eV) cerium oxide allows the activation of solar energy only within the UV range [23,24]. This can be used by doping ceria with transition metals such as Fe^{2+}, Mg^{2+}, Zr^{4+}, Zn^{2+}, Cu^{2+}, produced through a photocatalytic process with the production of electron-hole pairs [25]. Among these elements, Fe atoms have a lower bandwidth than cerium oxide and are capable of oxidizing more than other elements [26]. Therefore, it is necessary to transfer the absorption of CeO_2 to the visible region and reduce the recombination of electron-hole pairs. The application of this material and its properties are highly dependent on the quality and form of the powder. It is known that the synthesis method has a very important effect on the properties and quality of the powder. In recent years, as a result of the special properties of nanoparticles, the synthesis of nanopowders has been widely considered. For the synthesis of the CeO_2, various chemical treatments such as hydrothermal, chemical-chemical pyrolysis, combustible, sol-gel are used [27-32]. Among these methods, the coprecipitation method is very attractive due to the high speed and cheapness of raw materials. In the present study, FeCe magnetic nano-particles were

*Corresponding author. E-mail: farahmandjou@iauvaramin.ac.ir

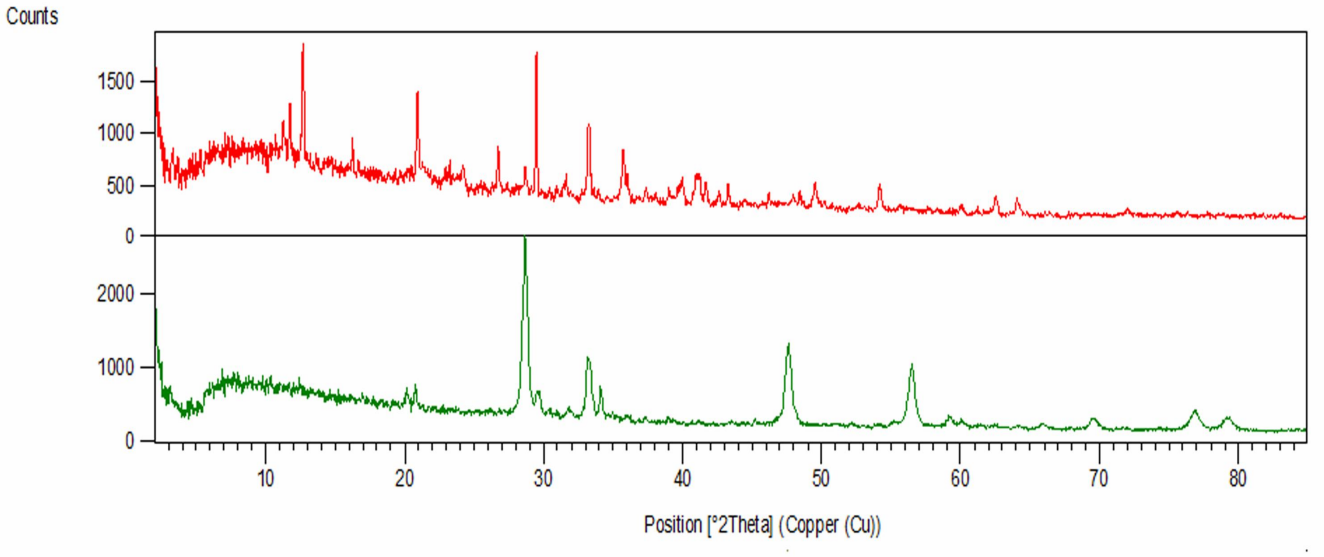

Fig. 1. XRD patterns of as-prepared and annealed FeCe samples.

synthesized using iron chloride and cerium chloride precursors in the presence of CTAB surfactant. Structural and surface morphological properties are evaluated by XRD, HRTEM, FESEM, EDS, VSM and FTIR analyses.

EXPERIMENTAL

In a typical experiment, 3 g $FeCl_3.6H_2O$ and 0.5 g CTAB was dissolved into 100 ml pure water under a magnetic stirrer. Thereafter, 3 g cerium chloride ($CeCl_2 \cdot 5H_2O$) was added to the solution with stirring at room temperature. After 10 min, the synthesis temperature was increased to 90 °C. In the first reaction, the pH = 4 and after 30 min at 90 °C, the pH reached 7. The products were evaporated for 3 h, cooled to room temperature and finally calcined at 500 °C for 4 h. All analyses were done for samples without any washing and purification.

The specification of the size, structure and optical properties of the as-synthesis and annealed nanoparticles were carried out. An x-ray diffractometer (XRD) was used to identify the crystalline phase and to estimate the crystalline size. The XRD pattern was recorded with 2θ in the range of 4-85° with type X-Pert Pro MPD, Cu-K_α: λ = 1.54 Å. The morphology was characterized by field emission scanning electron microscopy (SEM) with type KYKY-EM3200, 25 kV and transmission electron microscopy (TEM) with type Zeiss EM-900, 80 kV. Fourier transform infrared spectroscopy (FTIR) was conducted with WQF 510. Magnetic measurements were carried out using a vibration sampling magnetometer of type VSM 7400 Lake Shore. The Fe and Ce elemental analysis of the samples was performed by energy dispersive spectroscopy (EDS) type VEGA, 15 kV. All the measurements were carried out at room temperature.

RESULTS AND DISCUSSION

An x-ray diffractometer (XRD) with CuK_α radiation, operated at 40 kV, 250 mA was used to identify crystalline phases and to estimate the crystalline sizes. Figure 1 shows the x-ray diffraction patterns of the powder before and after heat treatment. Figure 1a shows the XRD pattern of Iron ceria sample before annealing. Figure 1b shows the XRD patterns of Iron cerium after annealing at 500 °C. The exhibited peaks correspond to the cubic structure. The mean size of the ordered FeCe nanoparticles has been estimated from full width at half maximum (FWHM), using Debye-Sherrer's formula [33] according to the following equation:

$$D = \frac{0.89\lambda}{B\cos\theta} \quad (1)$$

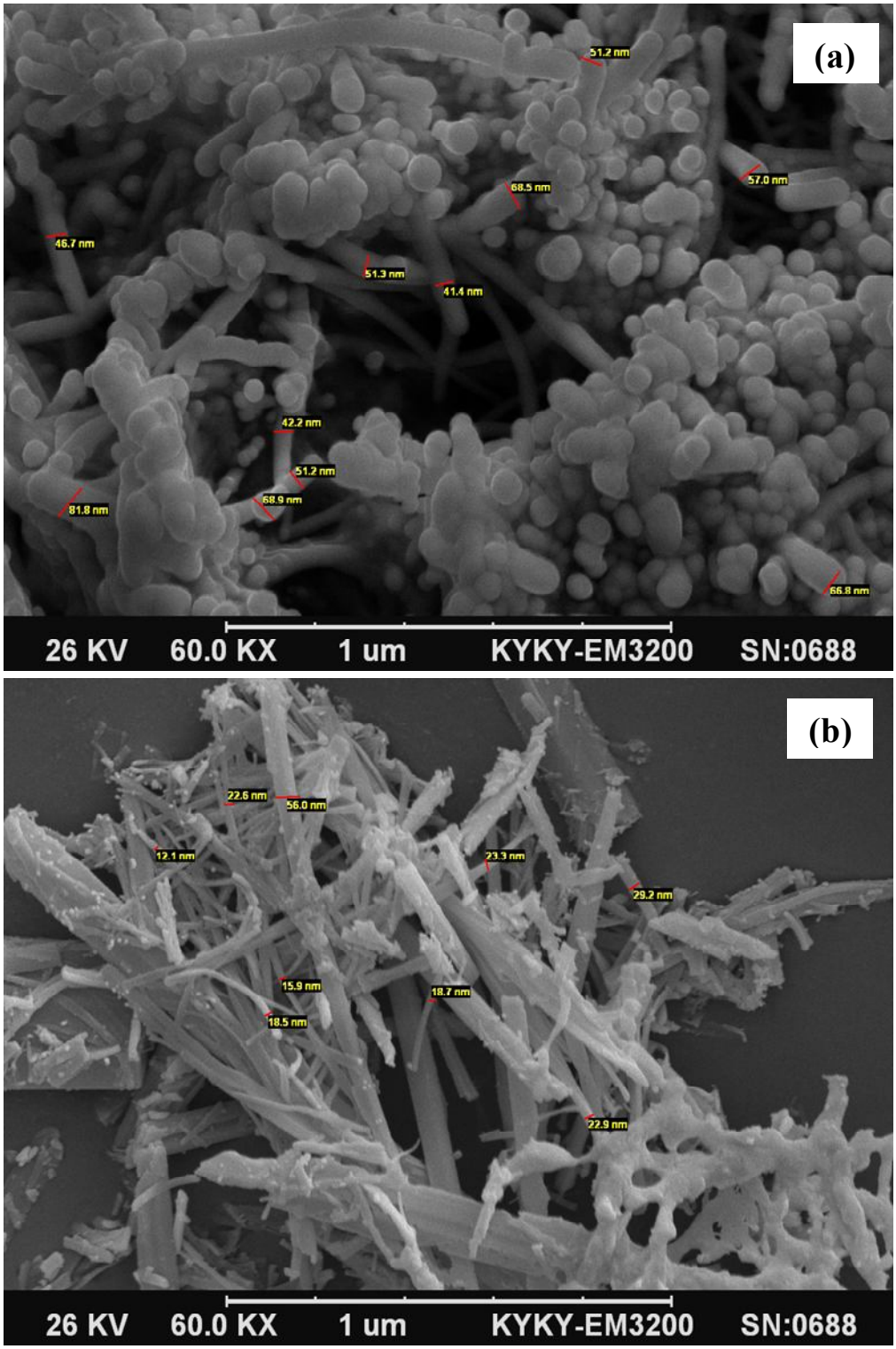

Fig. 2. SEM images of the (a) as-prepared (b) annealed FeCe nanoparticles at 500 °C.

Fig. 3. TEM image of the as-prepared FeCe nanoparticles.

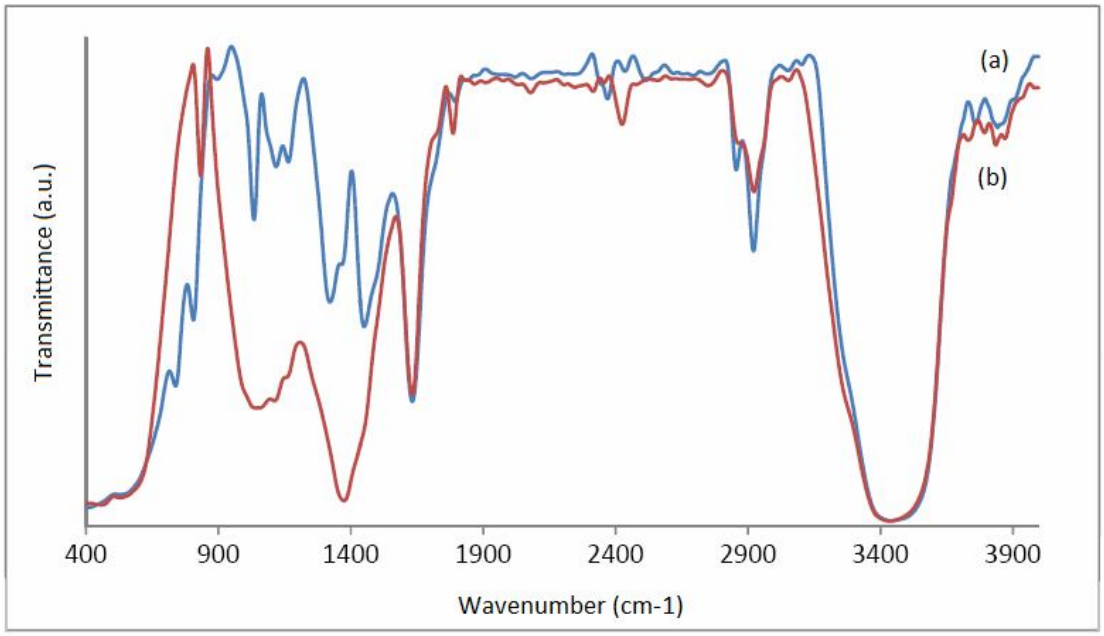

Fig. 4. FTIR spectrum of (a) as-prepared and (b) annealed FeCe samples.

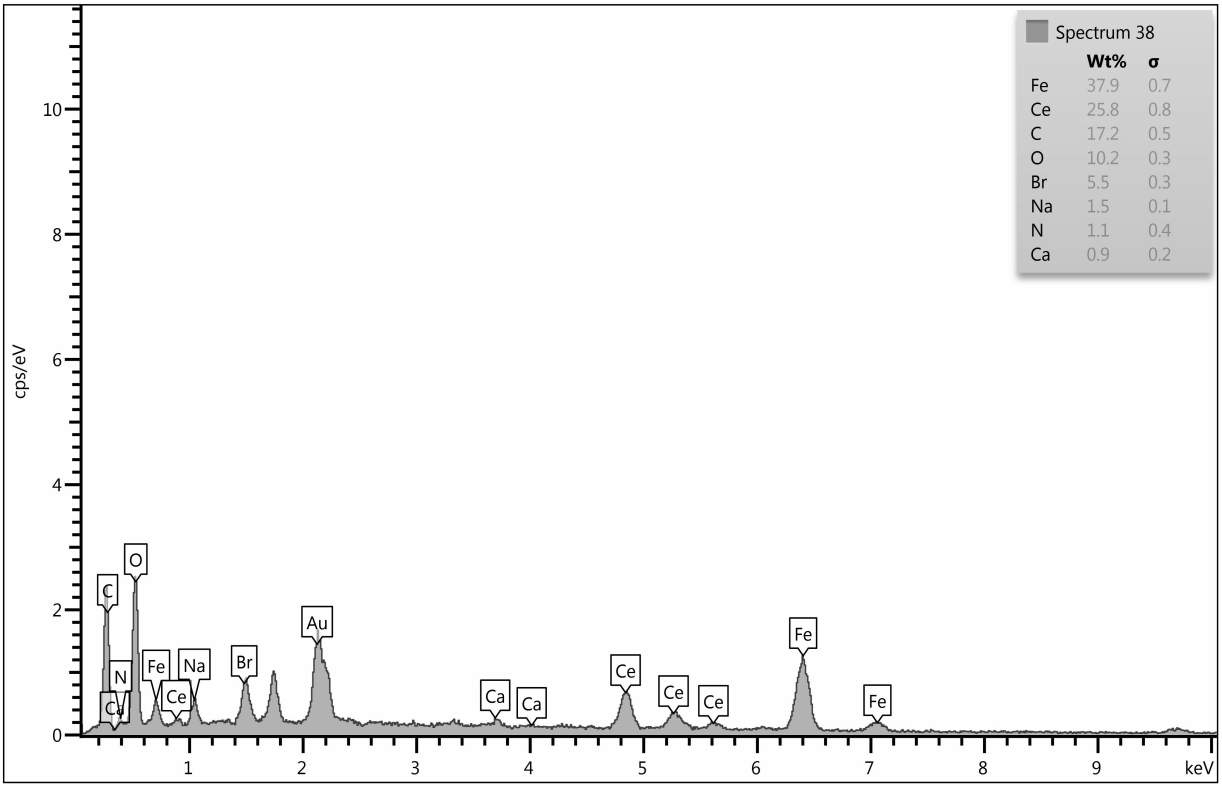

Fig. 5. EDS spectra of the as-synthesized FeCe prepared by wet synthesis.

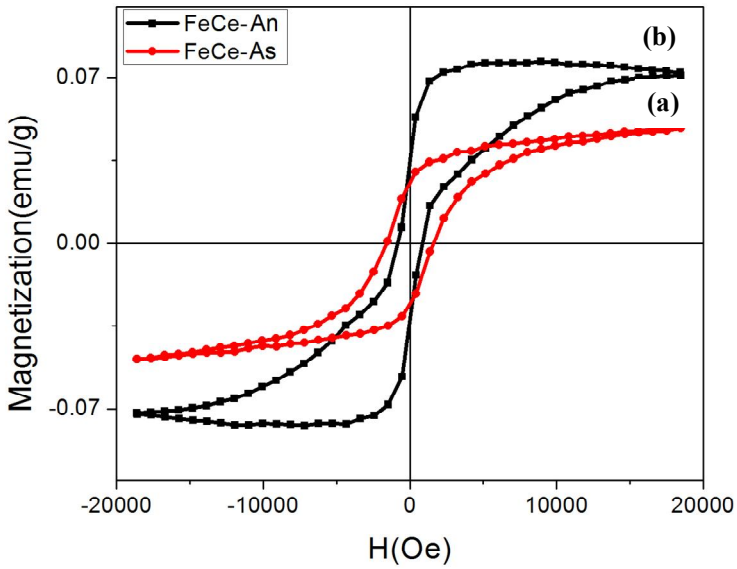

Fig. 6. Magnetic hysteresis loops at 300 K for representative iron cerium nanoparticles: (a) as-prepared, (b) annealed particles at 500 °C.

where, 0.89 is the shape factor, λ is the x-ray wavelength, B is the line broadening at half the maximum intensity (FWHM) in radians, and θ is the Bragg angle. From this Debye-Sherrer equation, The mean size of as-prepared samples was around 50 nm.

SEM analysis was used for the morphological study of the nanoparticles of samples. Figure 2a shows the SEM image of the as-prepared FeCe nanoparticles prepared by this method. In this figure, the particles were formed as rod-shaped with the formation of clusters. Figure 2b shows the SEM image of the annealed FeCe nanoparticles at 500 ^{o}C for 3 h. The particle size of as-prepared samples was measured in the range of 40-80 nm and the crystallite size of the annealed nanocrystals for the smallest one was about 15 nm in diameter.

The transmission electron microscopic (TEM) analysis was carried out to confirm the actual size of the particles, their growth pattern and the distribution of crystallites. Figure 3 shows the as-synthesized TEM image of squared-like FeCe nanoparticles with an average diameter of 50 nm, prepared by the chemical co-precipitation route.

In Fig. 4, the infrared spectrum (FTIR) of the as-synthesized and annealed FeCe nanoparticles are in the range of 400-4000 cm^{-1} wave number which identify the chemical bonds as well as functional groups in the compound. The large broad band at 3450 cm^{-1} is ascribed to the O-H stretching vibration in OH^- groups. The absorption peaks recorded around 1632 cm^{-1}, 1450 cm^{-1} are due to the asymmetric and symmetric bending vibrations of C=O. The strong band below 700 cm^{-1} is assigned the Fe-Ce stretching mode. The bands corresponding to the Fe-Ce stretching mode for as-prepared samples can be seen at 586 and 482 cm^{-1}.

Figure 5 shows the energy dispersive spectroscopy (EDS) of the FeCe sample prepared by wet synthesis. This confirms the existence of Fe and Ce by weight percent. EDS was used to analyze the chemical composition of a material under SEM. EDS shows the peaks of iron and cerium with fewer Bromide and sodium elements.

Magnetizations *M versus* applied magnetic field *H* for powders of the samples are measured at room temperature by cycling the magnetic field between -20k to 20k G. The magnetization curve in Fig. 7 shows the hysteresis behavior in the low field region. Figure 6a shows the coercive field and saturated magnetization around 1650 G and 0.04 emu g^{-1} respectively, for as-prepared sample while Fig. 6b shows the coercive field and saturated magnetization around 930 G and 0.07 emu g^{-1}, respectively, for the annealed one. It can be seen that the saturated magnetization increased with annealing temperature. The difference in M_S in the magnetic properties of Fe-doped CeO_2 materials depends on the preparation conditions such as temperature and atmosphere [34,35].

CONCLUSIONS

In the presence of CTAB surfactant, Fe-loaded ceria nanoparticles have been successfully synthesized using iron chloride and cerium chloride. The XRD spectrum shows the cubic structure of the samples. From the SEM images, it is clear that with increasing temperature, the size of the nanoparticles decreased with less agglomeration. The TEM image shows that the as-synthesized FeCe nanoparticles have an average diameter of about 50 nm with good uniformity. From the FTIR data, the presence of the Fe-Ce stretching mode can be seen. The EDS spectrum showed peaks of iron and cerium with less impurity. Magnetic measurements studies showed a magnetic coercive field and saturated magnetization around 1650 G and 0.04 emu g^{-1}, respectively.

ACKNOWLEDGMENTS

The authors are thankful for the financial support of Varamin Pishva branch at Islamic Azad University for analysis and the discussions on the results.

REFERENCES

[1] Farahmandjou, M.; Soflaee, F., Synthesis and characterization of α-Fe_2O_3 nanoparticles by simple co-precipitation method. *Phys. Chem. Res.* **2015**, *3*, 193-198, DOI: 10.22036/pcr.2015.9193.

[2] Farahmandjou, M.; Ramezani, M., Fabrication and characterization of rutile TiO_2 nanocrystals by water soluble precursor. *Phys. Chem. Res.* **2015**, *3*, 293-298, DOI: 10.22036/pcr.2015.10641.

[3] Shadrokh, S.; Farahmandjou, M.; Firozabadi, T. P.,

Fabrication and characterization of nanoporous Co oxide (Co_3O_4) prepared by simple sol-gel synthesis. *Phys. Chem. Res.* **2016**, *4*, 153-160, DOI: 10.22036/pcr.2016.12909.

[4] Farahmandjoua, M.; Honarbakhsha, S.; Behrouziniab, S., PVP-assisted synthesis of cobalt ferrite ($CoFe_2O_4$) nanorods. *Phys. Chem. Res.* **2016**, *4*, 655-662, DOI: 10.22036/pcr.2016.16702.

[5] Zarinkamar, M.; Farahmandjou, M.; Firoozabadi, T. P., Diethylene glycol-mediated synthesis of nano-sized ceria (CeO_2) catalyst. *J. Nanostruct.* **2016**, *6*, 114-118, DOI: 10.7508/jns.2016.02.002.

[6] Farahmandjou, M., Magnetocrystalline properties of Iron-Platinum (L10-FePt) nanoparticles through phase transition. *Iran. J. Phys. Res.* **2016**, *16*, 1-5, DOI: 10.18869/acadpub.ijpr.16.1.1.

[7] Honarbakhsh, S.; Farahmandjou, M.; Behroozinia, S., Synthesis and characterization of iron cobalt (FeCo) nanorods prepared by simple Co-precipitation method. *J. Fundam. Appl. Sci.* **2016**, *8*, 892-900, DOI: 10.4314/jfas.v8i2s.142.

[8] Farahmandjou, M.; Khalili, P., Morphology study of anatase nano-TiO_2 for self-cleaning coating. *Int. J. Fund. Phys. Sci.* **2013**, *3*, 54-56, DOI: 10.14331/ijfps.2013.330055.

[9] Farahmandjou, M., Synthesis of ITO nanoparticles prepared by degradation of sulfide method. *Chin. Phys. Lett.* **2012**, *29*, 077306-077309, DOI: 10.1088/0256-307X/29/7/077306.

[10] Farahmandjou, M., Two step growth process of iron-platinum (FePt) nanoparticles. *Int. J. Phys. Sci.,* **2012**, *7*, 2713-2719, DOI: 10.5897/IJPS11.1456.

[11] Farahmandjou, M., Synthesis and structural study of L10-FePt nanoparticles. *Turk. J. Engin. Environ. Sci.* **2010**, *34*, 265-270. DOI: 10.3906/muh-1010-20.

[12] Akhtari, F.; Zorriasatein, S.; Farahmandjou, M.; Elahi, S. M., Structural, optical, thermoelectrical, and magnetic study of $Zn_{1-x}Co_xO$ ($0 \leq x \leq 0.10$) nanocrystals. *Int. J. Appl. Ceram. Technol.* **2018**; *15*, 723-733, DOI: 10.1111/ ijac.12848.

[13] Akhtari, F.; Zorriasatein, S.; Farahmandjou, M.; Elahi, S.M., Synthesis and optical properties of Co^{2+}-doped ZnO Network prepared by new precursors. *Mater. Res. Express*. **2018**, *5*, 065015, DOI: 10.1088/2053-1591/aac6f1.

[14] Khoshnevisan, B.; Marami, M. B.; Farahmandjou, M., Fe^{3+}-Doped anatase TiO_2 study prepared by new sol-gel precursors. *Chin. Phys. Lett.* **2018**, *35*, 027501-027505, DOI: 10.1088/0256-307X/35/2/027501.

[15] Marami, M. B.; Farahmandjou, M.; Khoshnevisan, B., Solgel synthesis of Fe-doped TiO_2 nanocrystals. *J. Electron. Mater.* **2018**, *47*, 3741-3749, DOI: 10.1007/s11664-018-6234-5.

[16] Jafari, A.; Khademi, S.; Farahmandjou, M., Nano-crystalline Ce-doped TiO_2 powders: Sol-gel synthesis and optoelectronic properties. *Mater. Res. Express.* **2018**, *5*, 095008, DOI: 10.1088/2053-1591/aad5b5.

[17] Farahmandjou, M.; Honarbakhsh, S.; Behrouzinia, S., FeCo nanorods preparation using new chemical Synthesis. *J. Supercond. Nov. Magn.* **2018**, Accepted, DOI: 10.1007/s10948-018-4659-y.

[18] Khodadadi, A.; Farahmandjou, M.; Yaghoubi, M.; Amani, A.R., Structural and optical study of Fe^{3+}-doped Al_2O_3 nanocrystals prepared by new sol gel precursors. *Int. J. Appl. Ceram. Technol.* **2018**, Accepted, DOI:10.1111/ijac.13065.

[19] Kubo, T.; Obayasi, H., Oxygen ion conduction of the fluorite-type Ce1- xLnxO_2-x/2 (Ln = lanthanoid element). *J. Electrochem. Soc.* **1975**, *122*, 142-147. DOI: 10.1149/1.2134143.

[20] Fornasiero, P.; Balducci, G.; DiMonte, R.; Kaspar, J.; Sergo, V.; Gubitosa, G.; Ferrero, A.; Maziani, G., Modification of the redox behaviour of CeO_2 induced by structural doping with ZrO_2. *J. Catal.* **1996**, *164*: 173-183, DOI: 10.1006/jcat.1996.0373.

[21] Hirano, M.; Inagaki, M., Preparation of monodispersed cerium(IV) oxide particles by thermal hydrolysis: influence of the presence of urea and Gd doping on their morphology and growth. *J. Mater. Chem.* **2000**, *10*, 473-477, DOI: 10.1039/A907510K.

[22] Inaba, H.; Tagawa, H., Ceria-based solid electrolytes. *Solid State Ionics.* **1996**, *83*, 1-16, DOI: 10.1016/0167-2738(95)00229-4.

[23] Ho, C.; Yu, J. C.; Kwong, T.; Mak, A. C.; Lai, S., Morphology controllable synthesis of mesoporous CeO2 nano- and microstructures. *Chem. Mater.* **2005**, *17*, 4514-4522, DOI: 10.1021/cm0507967.

[24] Litter, M. I., Heterogeneous photocatalysis: transition metal ions in photocatalytic systems. *Appl. Catal. B.* **1999**, *23*, 89-114, DOI: 10.1016/S0926-3373(99)00069-7.

[25] Steele, B. C. H., Appraisal of Ce1-yGdyO_2−y/2 electrolytes for IT-SOFC operation at 500 °C. S*olid State Ionics.* **2000**, *129*, 95-110, DOI: 10.1016/S0167-2738(99)00319-7.

[26] Dastpak, M., Farahmandjou, M.; Firoozabadi, T. P., Synthesis and preparation of magnetic Fe-doped CeO_2 nanoparticles prepared by simple sol-gel method. *J. Supercond. Nov. Magn.* **2016**, *29*, 849-854, DOI: 10.1007/s10948-016-3639-3.

[27] Vanherle, J.; Horita, T.; Kawada, T.; Sakai, N.; Yokokawa, H.; Dokiya, M., Fabrication and sintering of fine yttria-doped ceria powder. *J. Am. Ceram. Soc.* **1997**, *80*, 933-940, DOI: 10.1111/j.1151-2916.1997.tb02924.x.

[28] Hirano, M.; Kato, E., Hydrothermal synthesis of nanocrystalline cerium(IV) oxide powders. *J. Am. Ceram. Soc.* **1999**, *82*, 786-788, DOI: 10.1111/j.1151-2916.1999.tb01838.x.

[29] Martinez-Arias, A.; Fernandez-Garcia, M.; Ballesteros, V.; Salamanca, L. N.; Conesa, J. C.; Otero, C.; Soria, J., Characterization of high surface area Zr-Ce (1:1) mixed oxide prepared by amicroemulsion method. *Langmuir,* **1999**, *15*, 4796-4802, DOI: 10.1021/la981537h.

[30] Li, L.; Lin, X.; Li, G.; Inomata, H., Solid solubility and transport properties of Ce1-xNdxO_2-δ nanocrystalline solid solutions by a sol-gel route. *J. Mater. Res.* **2001**, *16*, 3207-3213, DOI: 10.1557/JMR.2001.0442.

[31] Bera, P.; Aruna, S. T.; Patil, K. C.; Hegde, M. S., Studies on Cu/CeO_2: A new NO reduction catalyst. *J. Catal.* **1999**, *186*, 36-44, DOI: 10.1006/jcat.1999.2532.

[32] Zhou, Y.; Phillips, R.; Switzer, J. A., Electrochemical synthesis and sintering of nanocrystalline cerium(IV) oxide powders. *J. Am. Ceram. Soc.* **1995**, *78*, 981-985, DOI: 10.1111/j.1151-2916.1995.tb08425.x.

[33] Scherrer, P., Bestimmung der grosse und der inneren struktur von kolloidteilchen mittels rontgenstrahlen, nachrichten von der gesellschaft der wissenschaften. *Gottingen. Mathematisch-Physikalische Klasse.* **1918**, *2*, 98-100. DOI: 10.4236/health.2011.37070 2,486.

[34] Maensiri, S.; Phokha, S.; Laokul, P.; Seraphin, S., Room temperature ferromagnetism in Fe-Doped CeO2 nanoparticles. *J. Nanosci. Nanotechnol.* **2009**, *9*, 6415-6420, DOI: 10.1166/jnn.2009.1372.

[35] Coey, J. M. D.; Venkatesan, M.; Fitzerald, C. B., Donor impurity band exchange in dilute ferromagnetic oxides. *Nat. Mater.* **2005**, *4*, 173-179, DOI: 10.1038/nmat1310.